Mechanical response of plectonemic DNA: an analytical solution

N. Clauvelin, B. Audoly, S. Neukirch
UPMC Univ. Paris 06 & CNRS,
Institut Jean le Rond d'Alembert,
4, place Jussieu, Paris, France

February 21, 2008

Abstract

We consider an elastic rod model for twisted DNA in the plectonemic regime. The molecule is treated as an impenetrable tube with an effective, adjustable radius. The model is solved analytically and we derive formulas for the contact pressure, twisting moment and geometrical parameters of the supercoiled region. We apply our model to magnetic tweezer experiments of a DNA molecule subjected to a tensile force and a torque, and extract mechanical and geometrical quantities from the linear part of the experimental response curve. These reconstructed values are derived in a self-contained manner, and are found to be consistent with those available in the literature.

1 Introduction

Mechanical properties of the DNA molecule play an important role in the biological processes involved in the cell, yet we only have an imprecise view of these properties. Advances in nanotechnologies make it possible to exert forces onto isolated DNA filaments: mechanical response of the molecule is now widely studied. Single molecule experiments provide a powerful way to investigate the behavior of DNA subjected to mechanical stress. In such experiments, the molecule is held by optical or magnetic tweezers and forces and torques are applied to it [28, 8]. The interaction between DNA and proteins is actively investigated; for instance, the chemical and mechanical action of an enzyme on a molecule can be inferred from the global deformation of the molecule [24].

In this paper we focus on a specific type of experiments: a double stranded DNA molecule is fixed by one end to a glass surface while the other end is attached to a magnetic bead; using a magnet, a pulling force and a torque are applied on the DNA filament [30]. Large ranges of pulling

forces, from one tenth to one hundred piconewton, and number of turns can be explored in the experiments, and the molecule displays a variety of behaviors and conformations [1, 27, 7]. We study the response of the molecule to moderate forces, below 10 pN, and moderate to large number of turns, equivalent to a positive supercoiling ratio of the order of 0.1. In experiments, the pulling force is kept constant while the bead is rotated gradually. The vertical extension of the molecule is recorded and plotted as a function of the number of turns. Experimental rotation-extension curves have a characteristic shape and are called *hat curves* [5, 29]. At zero number of turns these curves exhibit a maximum, the value of which is explained by the worm-like chain (WLC) model [18] and its variants. For small number of turns the vertical extension decreases and the curve takes a rounded shape. Above a threshold value of the number of turns, the extension of the molecule decreases linearly. This linear part of the curve is obtained when the molecule wraps around itself in a helical way, giving rise to a structure comprising plectonemes. The plectonemic structure is made of two interwound helical filaments whose geometry is characterized by the so-called superhelical angle and radius; note that each of these filaments is itself made of a double-stranded DNA molecule. The superhelical angle and the twisting moment in the filaments are key parameters that control the action of topoisomerases [12], RNA polymerase [23], or other enzymes [32] on DNA. The distance of self-approach of DNA in supercoiled regime has been the subject of a number of studies [3, 25, 26, 9]. In previous analytical and numerical work, the double stranded DNA molecule has been modeled as a twist-storing elastic filament. These approaches have been successful at reproducing the response of DNA to moderate torque [4, 19], given by the central region of the experimental curves. The analysis of the linear regions of these curves, based on a detailed model of plectonemes, was lacking until recently: in Ref. [17], a composite model based on an empirical free energy of supercoiled DNA is proposed.

Here we present an elastic rod model for helical supercoiling of the DNA molecule, which is relevant to large number of turns. Our model is self-contained and provides a mechanically accurate description of elastic filaments in contact. The molecule is divided in two domains: one where the configuration is a worm-like-chain, dominated by thermal fluctuations, and the other one, a superhelical region dominated by elasticity, where the molecule contacts itself. Several plectonemic regions may lie at various places of the molecule, but as this does not change the mechanical response of the system, we refer to these regions as if they were in one piece. We deal with self-contact by introducing an effective superhelical radius (distinct from the crystallographic radius of 1 nm, from the size of the Manning condensate and from the Debye length, although in the same range of values), which varies with external loads and salinity of the solution. The effective radius is defined as the radius of a chargeless, impenetrable and elastic

tube having the same mechanical response as the molecule. This radius is not given as a parameter of the model and is extracted from experimental data. Using an energy approach, we relate geometrical variables (superhelical radius and angle) to applied force and torque. We also characterize the response of the molecule in the plectonemic regime, extend former numerical results [20], and show how geometrical and mechanical parameters can be extracted from experimental data.

2 Model

The present model investigates the equilibrium behavior of an elastic rod with bending rigidity K_0 (the bending persistence length is $A = K_0/(kT)$, where k is the Boltzmann constant and T the absolute temperature) and twisting rigidity K_3 under traction and torsion as shown in Fig. 1. This is a coarse-grained model for DNA where base-pairs details are neglected. For instance, the anisotropic flexibility of the molecule, originating from base pairing and major-minor grove geometry, is smoothed out at a scale of several base pairs: a highly twisted anisotropic rod can be replaced by an equivalent isotropic rod with effective bending rigidity [11].

Geometry

We start with a geometric description of the rod configurations relevant to the plectonemic regime. This defines a reduced set of configurations (Ansatz), over which we shall minimize the elastic strain energy associated with deformations. The rod, of length ℓ, is considered inextensible and has circular cross-section; let s denote the arclength along the rod. The strain energy involves, at lowest order, the geometric curvature $\kappa(s)$ of the centerline of the rod as well as the twist $\tau(s)$. We emphasize that the twist $\tau(s)$ is different from the geometrical (Frénet-Serret) torsion of the centerline as it takes into account the rotation of material cross-sections around the centerline. It allows one to distinguish between twisted and untwisted configurations of the rod having the same centerline. The rod centerline is parameterized by $\mathbf{r}(s)$ and its unit tangent $\mathbf{t} \stackrel{\text{def}}{=} \mathrm{d}\mathbf{r}/\mathrm{d}s$ can be described with spherical angles, as shown in Fig. 1: $\alpha(s)$ is the zenith angle and $\psi(s)$ the azimuth angle with respect to the direction $\mathbf{e_x}$ along the common axis of the two superhelices in the plectonemic region.

We consider the following configurations, relevant to a large applied number of turns, n. The tails are assumed to be straight but twisted (thermal fluctuations will be accounted for by using the rescaled tail length predicted by WLC theory). The plectonemes are described by two identical and uniform helices where, again, each of these helices is itself a double-stranded DNA molecule. Both the end loop of the plectonemes and the matching

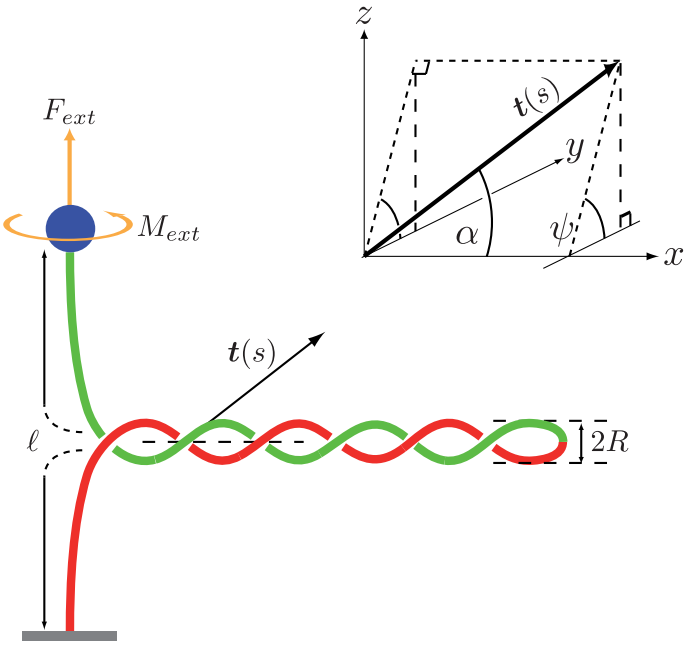

Figure 1: Sketch of the magnetic tweezers experiment. A B-DNA molecule of total contour length ℓ is fixed in $s = 0$ to a glass surface while the other end in $s = \ell$ is attached to a magnetic bead. A pulling force F_{ext} and a torque M_{ext} are applied at the upper end by using a magnet. The superhelical angle and radius are denoted α and R respectively. The zenith angle α and the azimuth angle ψ of the tangent vector with regard to the superhelical axis $\mathbf{e_x}$ are also shown.

region between the tails and the plectonemic part are neglected. Consequently the rod comprises two phases: one made up of straight and twisted tails and the other one of plectonemic structures. The plectonemic phase is not necessarily made of a single component but, for the sake of simplicity, we discuss the case of a single plectonemic structure (our results are still valid if the plectonemes are split into several components).

In the tails the rod is straight and aligned with the $\mathbf{e_z}$ axis: $\mathbf{t} = \mathbf{e_z}$. The geometric curvature $\kappa \stackrel{\text{def}}{=} |\mathrm{d}\mathbf{t}/\mathrm{d}s|$ is zero, $\kappa(s) = 0$.

In each filament of the plectonemes, the position vector $\mathbf{r}(s)$ and the tangent vector $\mathbf{t}(s)$ describe a superhelix of axis $\mathbf{e_x}$:

$$\begin{cases} r_x(s) = s\,\cos\alpha \\ r_y(s) = \chi\,R\,\sin\psi(s) \\ r_z(s) = -\chi\,R\,\cos\psi(s) \end{cases} \quad \text{and} \quad \begin{cases} t_x(s) = \cos\alpha \\ t_y(s) = \sin\alpha\,\cos\psi(s) \\ t_z(s) = \sin\alpha\,\sin\psi(s) \end{cases} \tag{1}$$

The other filament of the plectonemes is obtained by a rotation of 180° around the axis $\mathbf{e_x}$. Here $\chi = \pm 1$ stands for the chirality of the two helices and R and α denote the superhelical radius and angle, respectively. In equation (1), the condition $\mathrm{d}\mathbf{r}/\mathrm{d}s = \mathbf{t}$ yields $\mathrm{d}\psi/\mathrm{d}s = \chi\,\sin\alpha/R$. The curvature in the plectonemes is $\kappa(s) \stackrel{\text{def}}{=} |\mathrm{d}\mathbf{t}/\mathrm{d}s| = \frac{\sin^2\alpha}{R}$.

Noting ℓ_p the contour length spent in the plectonemes, we obtain the following expression for the integral of the squared curvature over the whole length of the rod:

$$\int_0^\ell \kappa^2\,\mathrm{d}s = \frac{\sin^4\alpha}{R^2}\,\ell_\mathrm{p}. \tag{2}$$

The end torque twists the filament. For a rod with circular cross-section, the twist $\tau(s)$ at equilibrium is uniform [2], $\mathrm{d}\tau/\mathrm{d}s = 0$ for all s. As a result, the equilibrium configuration of the rod is fully specified by the centerline, through the variables α, R and ℓ_p, and an additional scalar τ describing twist.

The twist τ is geometrically related to the number of turns imposed on the magnetic bead, n, which is equal to the link of the DNA molecule, $n = \mathrm{Lk}$. In the present case the link reads [20]:

$$\mathrm{Lk} = \mathrm{Tw} + \mathrm{Wr} = \frac{1}{2\pi}\int_0^\ell \tau\,\mathrm{d}s - \chi\,\frac{\sin 2\alpha}{4\pi\,R}\,\ell_p = \frac{1}{2\pi}\left(\tau\,\ell - \chi\,\frac{\sin 2\alpha}{2\,R}\,\ell_\mathrm{p}\right), \tag{3}$$

as we neglect the writhe of the tails.

Energy formulation

Using the above notations the rod is described by four variables: α the superhelical angle, R the superhelical radius, τ the twist and ℓ_p the contour length spent in the plectonemes. We proceed to derive the total energy

of the system as a function of these four variables. It is the sum of three terms, $V = V_{\rm el} + V_{\rm ext} + V_{\rm int}$, where the first term is the strain elastic energy, the second is the potential energy associated with the external loads $F_{\rm ext}$ and $M_{\rm ext}$, and the third accounts for interaction of the filaments in the plectonemes. The strain elastic energy for the rod of total contour length ℓ is :

$$V_{\rm el} = \frac{K_0}{2}\int_0^\ell \kappa^2\,{\rm d}s + \frac{K_3}{2}\int_0^\ell \tau^2\,{\rm d}s\ . \tag{4}$$

We do not take into account the reduction of the effective torsional rigidity in the tails due to fluctuations [19]. The potential energy is given by:

$$V_{\rm ext} = -F_{\rm ext}(z(\ell) - z(0)) - 2\pi\, M_{\rm ext}\, n\ , \tag{5}$$

where $z(\ell) - z(0) = \ell - \ell_p$ for straight tails and $n = {\rm Lk}$.

If the DNA-DNA interaction was clearly established, we would include the corresponding interaction energy $V_{\rm int}$ in the total energy V [10]. This is not the case and we model the filaments in electrostatic interaction as effective chargeless hard-core tubes. The effective radius a of these tubes accounts for a variety of physical mechanisms, including for example the presence of counter-ions or thermal fluctuations in the plectonemes, which we do not attempt to model. As in Refs. [33, 25], we do not try to predict the actual radius a but simply follow its variation under changing experimental conditions (applied load, salinity, etc.). Doing so, we replace the actual (unknown) interaction potential $V_{\rm int}(R, \alpha)$ by a hard-core interaction with adjustable radius a, and optimize a to best fit a given experiment. In section 3 we show how a can be extracted from experimental measurements.

The parameter a must certainly be larger than the crystallographic DNA radius 1 nm. It is different from the radius of the Manning condensate [14, 15, 16] since approximately a quarter of the charge remains outside of the Manning condensate. The equilibrium is the solution of a constrained minimization problem for the elastic energy, subjected to the impenetrability condition

$$R \geq a. \tag{6}$$

We anticipate on the fact that there is contact, $R = a$, for typical experimental conditions. Consequently we replace the actual interaction energy with a constraint term:

$$V_{\rm int} = -\lambda\,(R - a)\,, \tag{7}$$

where λ is a Lagrange multiplier. Note that this term is not a regular energy but comes from the constraint: the multiplier λ has to be set at the end of the procedure and chosen in such a way that the constraint $R = a$ is satisfied.

Combining Eqs. (2–7), we write the total potential energy of the system

as:

$$V(\alpha, R, \tau, \ell_{\rm p}) = \frac{K_0}{2}\,\frac{\sin^4\alpha}{R^2}\,\ell_p + \frac{K_3}{2}\,\tau^2\,\ell - F_{\rm ext}\,(\ell - \ell_{\rm p}) \\ - M_{\rm ext}\left(\tau\,\ell - \chi\,\frac{\sin 2\alpha}{2\,R}\,\ell_{\rm p}\right) - \lambda\,(R - a)\,. \quad (8)$$

In Ref. [13] a similar energy function has been introduced but the rest of analysis differs from ours. Indeed, their approach focuses on statistical mechanics and the analysis of the state of lowest energy is overlooked. Moreover, the parameter a is fixed a priori to the crystallographic radius of DNA, $a = 1$ nm, which is a strong restriction and an underestimation of the actual distance of self-approach of DNA in saline solution. In contrast, we undertake a detailed analysis of the equilibrium solutions, with thermal fluctuations considered in the tails; this allows us to derive simple formulas for the force and the moment as a function of the superhelical variables, applicable to magnetic tweezers experiments.

3 Results

Mechanical equilibrium is given by the Euler-Lagrange condition for the stationarity of the potential $V(\alpha, R, \tau, \ell_{\rm p})$ in Eq. (8) with respect to its variables,

$$\left(\frac{\partial V}{\partial \tau}, \frac{\partial V}{\partial \alpha}, \frac{\partial V}{\partial \ell_{\rm p}}, \frac{\partial V}{\partial R}\right) = 0.$$

The first condition $\partial V/\partial\tau$ allows one to recover the constitutive relation for twist deformations, $M_{\rm ext} = K_3\,\tau$, given that the twisting moment is uniform in the filament and equal to the applied torque $M_{\rm ext}$.

Variation of the total energy with respect to α gives the expression of the applied torque $M_{\rm ext}$ in terms of the superhelical variables α and R:

$$M_{\rm ext} = -\frac{2\chi\,K_0}{R}\,\frac{\cos\alpha\,\sin^3\alpha}{\cos 2\alpha}, \quad (9)$$

which is what was found for purely plectonemic solution (no tails) [31].

The condition $\partial V/\partial\ell_{\rm p} = 0$, combined with Eq. (9), allows one to relate the pulling force $F_{\rm ext}$ to the superhelical geometry:

$$F_{\rm ext} = \frac{K_0}{R^2}\,\sin^4\alpha\,\left(\frac{1}{2} + \frac{1}{\cos 2\alpha}\right). \quad (10)$$

This formula justifies and extends the numerical fit $F_{\rm ext} \propto K_0\,\alpha^4/R^2$ found in Ref. [20] for small values of α.

The Euler-Lagrange condition with respect to R yields an equation involving the Lagrange multiplier λ. The quantity $\lambda/\ell_{\rm p}$ can be interpreted as

the contact force per unit length, p, of one filament onto the other. Eqs. (8–9), together with the condition $\partial V/\partial R = 0$, yields:

$$p = \frac{\lambda}{\ell_p} = \frac{K_0}{R^3}\frac{\sin^4\alpha}{\cos 2\alpha}. \tag{11}$$

Note that this pressure (more accurately, force per unit length) is positive for $\alpha \leq \pi/4$; if our assumption of contact $R = a$ was incorrect, this would be indicated by a negative pressure value here.

In magnetic tweezers experiments, the pulling force F_{ext} is imposed although the applied torque M_{ext} is unknown. The two unknowns R and α are then related by Eq. (10); in the next Section, a second equation relating those unknowns and the extension z is given, which makes it possible to solve for R and α. The twisting moment can then be found from Eq. (9).

Vertical extension of the filament

In magnetic tweezers experiments, the measurable quantities are the vertical extension z and the number of turns n imposed on the bead. Using Eq. (3) for $n = \text{Lk}$, the equation $z = \ell - \ell_{\text{p}}$ and the constitutive relation $\tau = M_{\text{ext}}/K_3$ where M_{ext} is found from Eq. (9), we obtain the vertical extension of the filament as a linear function of the number of turns n:

$$z = \left(1 + \frac{2\,K_0}{K_3}\frac{\sin^2\alpha}{\cos 2\alpha}\right)\ell + \chi\, n\,\frac{4\pi\, R}{\sin 2\alpha}\ . \tag{12}$$

Thermal fluctuations dominantly affect the tails and make the end-to-end distance z of the molecule smaller than the contour length $\ell - \ell_{\text{p}}$ of the tail parts, by a factor $\rho_{\text{wlc}} \in [0, 1]$: $z = \rho_{\text{wlc}}\,(\ell - \ell_{\text{p}})$. This factor depends on both the pulling force F_{ext} and the bending persistence length $A = K_0/(kT)$ and can either be read off an experimental hat curve from the value $z(n = 0) = \rho_{\text{wlc}}\,\ell$, or computed from theoretical formulas [18, 6]. The dependence of ρ_{wlc} on the pulling force makes the tails effectively extensible (this is the classical entropic stiffness of a chain). To account for these thermal effects, we replace Eq. (12) with:

$$z = \rho_{\text{wlc}}\left(1 + \frac{2\,K_0}{K_3}\frac{\sin^2\alpha}{\cos 2\alpha}\right)\ell + \chi\,\rho_{\text{wlc}}\,\frac{4\pi\, R}{\sin 2\alpha}\,n\ . \tag{13}$$

One of the main features of the experimental hat curves is the linear decrease of the vertical extension with the number of turns. We define the slope q in the linear part of the hat curve as:

$$q \stackrel{\text{def}}{=} \left|\frac{\mathrm{d}z}{\mathrm{d}n}\right| = \rho_{\text{wlc}}\frac{4\pi\, R}{\sin 2\alpha}\ . \tag{14}$$

Given experimental values of F_{ext} and q, Eqs. (10) and (14) can be solved for R and α. Since q (and F_{ext}) are constant along the linear part of a hat

curve, the values of R and α thus determined will be constant as well. As a result, the twisting moment in the molecule, given by Eq. (9), is constant, for a given experiment, along the linear region of the hat curve, a property that has been previously reported in the literature [5, 17] and which is a clear outcome of the present model. An interpretation of the fact that R and α are constant in the linear region of the hat curve is that each additional turn of the bead is used to convert a small piece of tail into plectonemes.

Twisting moment

The twisting moment in the molecule, which is uniform and equal to $M_{\rm ext}$ at equilibrium, cannot be measured in magnetic tweezers experiments. However, it has been shown that enzyme activity such as RNA polymerase depends on the value of the twisting moment in DNA [23]. The value of $M_{\rm ext}$ can be determined from Eq. (9) once R and α are known, as explained above. Here, we give a formula for $M_{\rm ext}$ directly as function of the experimental slope q and the external force $F_{\rm ext}$. Indeed, using Eq. (14) to eliminate R in Eqs. (9) and (10), one obtains $M_{\rm ext}(q,\alpha)$ and $F_{\rm ext}(q,\alpha)$ as functions of q and α. It is then possible to eliminate α, which yields:

$$M_{\rm ext} = m + \left(m^2 + 2K_0\, F_{\rm ext}\right)^{1/2}, \qquad \text{where } m = \frac{q\, F_{\rm ext}}{4\pi\, \rho_{\rm wlc}} - \frac{3\pi\, \rho_{\rm wlc}\, K_0}{2q} \quad (15)$$

In the limit of small α, one can expand the functions $M_{\rm ext}(q,\alpha)$ and $F_{\rm ext}(q,\alpha)$ prior to elimination of α, and this leads to a simplified formula:

$$M_{\rm ext} \simeq \frac{2\, q}{3\, \pi\, \rho_{\rm wlc}} F_{\rm ext}, \quad (16)$$

where, as explained above, $\rho_{\rm wlc} = z(n=0)/\ell$. As shown in Fig. 4, this approximation is accurate when used with typical experimental values. Eq. (16) provides a simple and direct mean of evaluating the twisting moment in magnetic tweezers experiments, based on the slope of the linear part of the hat curve only. Note that it should not be inferred from Eq. (16) that $M_{\rm ext}$ depends linearly on $F_{\rm ext}$, as the slope q is itself a function of $F_{\rm ext}$.

Superhelical angle limit

It is known that the topology of contact between two impenetrable helical tubes winding along a common axis changes when α becomes larger than $\pi/4$ [21]. The possibility of such a change of topology is not considered in our model (being specific to hard-core repulsion between tubes, it is not relevant to DNA molecules undergoing long-range electrostatic repulsion anyway). Nevertheless, the equilibrium solutions found here are all such that $\alpha < \pi/4$. This upper bound has a mechanical origin, and not a geometrical one: the expressions for $F_{\rm ext}$ in Eq. (10) and for $M_{\rm ext}$ in Eq. (9) both diverge

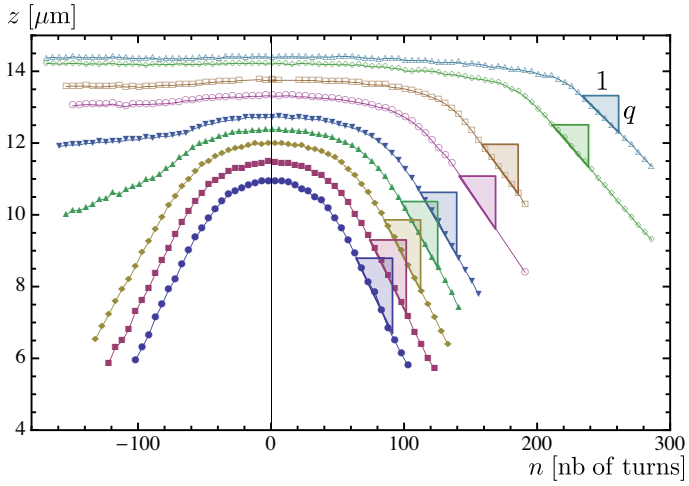

Figure 2: Experimental hat curves showing the vertical extension of a lambda phage DNA 48kbp molecule as a function of the number of turns imposed on the magnetic bead (salt concentration 10 mM, temperature 298 K). Experimentally measured persistence length of the molecule is $A = 51.35$ nm. Each curve corresponds to a fixed pulling force $F_{\rm ext}$: 0.25, 0.33, 0.44, 0.57, 0.74, 1.10, 1.31, 2.20, 2.95 pN. Triangles represent the fit for the slope q of the linear region. Data kindly provided by V. Croquette (CNRS, France).

at $\alpha = \pi/4$ and plectonemic solutions with a superhelical angle larger than $\pi/4$ are unstable.

Application to experiments

The model is used to extract mechanical and geometrical parameters from experimental data. To allow comparison with previous work, we use the same data as in [20]. These data are shown in Fig. 2; they were obtained on a 48kbp lambda phage DNA molecule in a 10mM phosphate buffer.

For each curve in Fig. 2, corresponding to a given value of the external force $F_{\rm ext}$, we extract the slope q by fitting the linear region. The superhelical variables R and α are found by solving Eqs. (10) and (14), and are plotted in Fig. 3 as a function of $F_{\rm ext}$. The reconstructed values of R are in the nanometric range; they decrease with the pulling force, from approximately 6 to 2 times the DNA crystallographic radius in this particular experiment. At large values of the force, R is close to (and actually smaller than) the Debye length, 3.07 nm in 10 mM salt, and the Manning condensation radius, 3.18 nm in 10 mM salt [22]. We note that the values of R found here in the presence of a pulling force are smaller than (and in the same range as) in

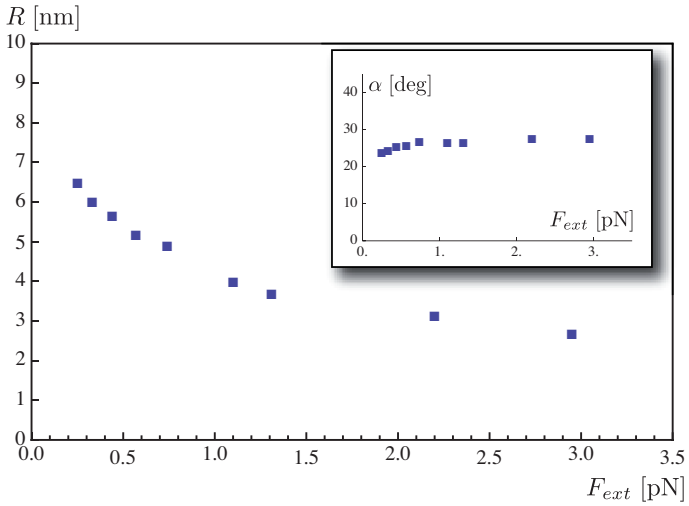

Figure 3: Reconstructed values of the plectonemic radius R as a function of the pulling force, from the data in Fig. 2 by solving Eqs. (10) and (14). The angle α is shown in the inset.

Ref. [26] where no force is applied, which is consistent.

The reconstructed values of the twisting moment $M_{\rm ext}$ and of the contact pressure p are given in Fig. 4, based on the same experimental data. The values of $M_{\rm ext}$ are determined both by Eq. (9) using the previously computed values of R and α, and by the approximate formula (16) directly. A good agreement is obtained, which validates the proposed approximation. The values of $M_{\rm ext}$ are also compared to those predicted by a composite analytical model, see Eq. (17) in Ref. [17] (this model uses effective parameters determined from Monte-Carlo simulations [34]).

4 Conclusion

We have shown that, under the approximation that thermal fluctuations are neglected in the plectonemes, one can calculate analytically the response of twisted DNA: supercoils are described by a mechanically exact and self-contained model. Self-contact in the plectonemic region is treated with a hard-core potential; an expression for the contact pressure between the two dsDNA is derived. The hard-core radius is an effective parameter determined, for a given value of the applied force, from the slope of the linear region of the experimental curve. A formula for the twisting moment is proposed, as a function of the slope of the linear region of the experimental hat curve only. We apply this analysis to experimental data from which we extract the mechanical quantities: superhelical radius and angle, contact

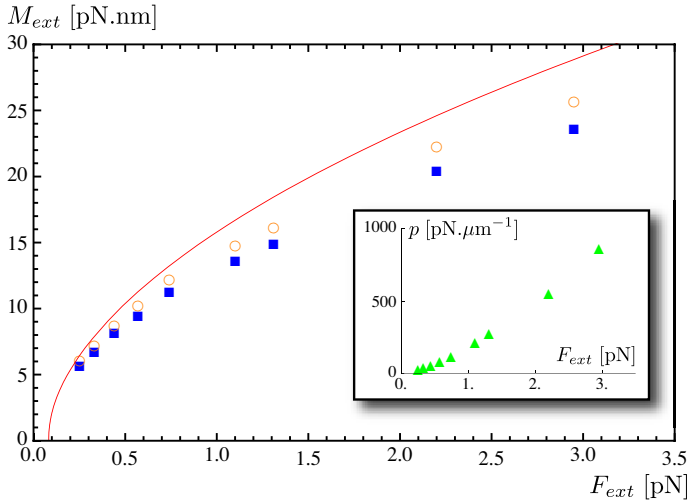

Figure 4: Reconstructed values for the twisting moment in the molecule based on the data shown in Fig. 2, using the exact formula in Eq. (9) (solid squares), and the small angles approximation in Eq. (16) (open circles). Comparison with the prediction of the composite model in Ref. [17] (curve). Contact pressure is shown in inset.

pressure and twisting moment. We compared these values with predictions from previous analyses, when available, and found that they are consistent. In future work, we shall extend the present model to deal with long-range interaction potentials, predict the superhelical radius, and utilize magnetic tweezers experiments to probe DNA-DNA electrostatic interaction. The present paper is a first step towards a mechanically accurate description of bare dsDNA subjected to tensile and torsional loads, a problem relevant to the architecture of DNA in the cell nucleus where proteins come into play.

Acknowledgment: We thank V. Croquette for providing us with the experimental data used here.

References

[1] J. F. Allemand, D. Bensimon, R. Lavery, and V. Croquette. Stretched and overwound DNA forms a pauling-like structure with exposed bases. *Proc. Natl . Acad. Sci . USA*, 95:14152–14157, 1998.

[2] S. S. Antman. *Nonlinear Problems of Elasticity*. Springer Verlag, New York, 2005.

[3] J. Bednar, P. Furrer, A. Stasiak, J. Dubochet, E. H. Egelman, and A. D. Bates. The twist, writhe and overall shape of supercoiled DNA change during counterion-induced transition from a loosely to a tightly interwound superhelix. possible implications for DNA structure in vivo. *J. Mol. Biol.*, 235(3):825–847, 1994.

[4] C. Bouchiat and M. Mézard. Elasticity model of a supercoiled DNA molecule. *Physical Review Letters*, 80(7):1556–1559, 1998.

[5] C. Bouchiat and M. Mézard. Elastic rod model of a supercoiled DNA molecule. *European Physical Journal E*, 2:377–402, 2000.

[6] C. Bouchiat, M. D. Wang, J.-F. Allemand, T. Strick, S. M. Block, and V. Croquette. Estimating the persistence length of a worm-like chain molecule from force-extension measurements. *Biophysical Journal*, 76:409–413, 1999.

[7] Zev Bryant, Michael D. Stone, Jeff Gore, Steven B. Smith, Nicholas R. Cozzarelli, and Carlos Bustamante. Structural transitions and elasticity from torque measurements on DNA. *Nature*, 424:338–341, 2003.

[8] C. Bustamente, J. F. Marko, E. D. Siggia, and S. Smith. Entropic elasticity of lambda-phage DNA. *Science*, 265:1599–1600, 1994.

[9] G. Charvin, A. Vologodskii, D. Bensimon, and V. Croquette. Braiding DNA: Experiments, simulations, and models. *Biophysical Journal*, 88:4124–4136, 2005.

[10] N. Clauvelin, B. Audoly, and S. Neukirch. Plectonemic DNA experiment to test longe-range interaction potential. submitted.

[11] S. Kehrbaum and J. H. Maddocks. Effective properties of elastic rods with high intrinsic twist. *Proceedings of the 16th IMACS World Congress*, 2000.

[12] Daniel A. Koster, Vincent Croquette, Cees Dekker, Stewart Shuman, and Nynke H. Dekker. Friction and torque govern the relaxation of DNA supercoils by eukaryotic topoisomerase IB. *Nature*, 434:671–674, 2005.

[13] S. Kutter and E. M. Terentjev. Helix coil mixing in twist-storing polymers. *European Physical Journal B*, 21:455–462, 2001.

[14] G. S. Manning. Limiting laws and counterion condensation in polyelectrolyte solutions - I. colligative properties. *Journal of Chemical Physics*, 51(3):924–933, 1969.

[15] G. S. Manning. Limiting laws and counterion condensation in polyelectrolyte solutions - II. self-diffusion of the small ions. *Journal of Chemical Physics*, 51(3):934–938, 1969.

[16] G. S. Manning. Limiting laws and counterion condensation in polyelectrolyte solutions - III. an analysis based on the mayer ionic solution theory. *Journal of Chemical Physics*, 51(8):3249–3252, 1969.

[17] J. F. Marko. Torque and dynamics of linking number relaxation in stretched supercoiled DNA. *Physical Review E*, 76:021926, 2007.

[18] J. F. Marko and E. D. Siggia. Streching DNA. *Macromolecules*, 28:8759–8770, 1995.

[19] J. David Moroz and Philip Nelson. Torsional directed walks, entropic elasticity, and DNA twist stiffness. *Proceedings of the National Academy of Sciences, USA*, 94:14418, 1997.

[20] S. Neukirch. Extracting DNA twist rigidity from experimental supercoiling data. *Physical Review Letters*, 93(19):198107, 2004.

[21] Sébastien Neukirch and Gert van der Heijden. Geometry and mechanics of uniform n-plies: from engineering ropes to biological filaments. *Journal of Elasticity*, 69:41–72, 2002.

[22] B. O'Shaughnessy and Q. Yang. Manning-Osawa counterion condensation. *Physical Review Letters*, 94(048302):1–4, 2005.

[23] Andrey Revyakin, Richard H. Ebright, and Terence R. Strick. Promoter unwinding and promoter clearance by RNA polymerase: Detection by single-molecule DNA nanomanipulation. *Proc. Natl. Acad. Sci. USA*, 101(14):4776–4780, 2004.

[24] Andrey Revyakin, Chenyu Liu, Richard H. Ebright, and Terence R. Strick. Abortive Initiation and Productive Initiation by RNA Polymerase Involve DNA Scrunching. *Science*, 314(5802):1139–1143, 2006.

[25] V. V. Rybenkov, A. V. Vologodskii, and N. R. Cozzarelli. The effect of ionic conditions on DNA helical repeat, effective diameter and free energy of supercoiling. *Nucleic Acids Research*, 25(7), 1997.

[26] Valentin V. Rybenkov, Nicholas R. Cozzarelli, and Alexander V. Vologodskii. Probability of DNA knotting and the effective diameter of the DNA double-helix. *Proc. Natl. Acad. Sci. USA*, 90:5307–5311, 1993.

[27] A. Sarkar, J. F. Leger, D. Chatenay, and J. F. Marko. Structural transitions in DNA driven by external force and torque. *Physical Review E*, 63:051903, 2001.

[28] S. B. Smith, L. Finzi, and C. Bustamante. Direct mechanical measurements of the elasticity of single DNA molecules by using magnetic beads. *Science*, 258:1122–1126, 1992.

[29] T. Strick, J.-F. Allemand, D. Bensimon, and V. Croquette. Behavior of supercoiled DNA. *Biophysical Journal*, 74(2016–2028), 1998.

[30] T. R. Strick, J.-F. Allemand, D. Bensimon, A. Bensimon, and V. Croquette. The elasticity of a single supercoiled DNA molecule. *Science*, 271:1835–1837, 1996.

[31] J. M. T. Thompson, G. H. M. van der Heijden, and S. Neukirch. Supercoiling of DNA plasmids: mechanics of the generalized ply. *Proc. R. Soc. Lond. A*, 458:959–985, 2002.

[32] Thijn van der Heijden, John van Noort, Hendrikje van Leest, Roland Kanaar, Claire Wyman, Nynke Dekker, and Cees Dekker. Torque-limited RecA polymerization on dsDNA. *Nucleic Acids Research*, 33(7):2099–2105, 2005.

[33] Alexander Vologodskii and Nicholas Cozzarelli. Modeling of long-range electrostatic interactions in DNA. *Biopolymers*, 35(3):289–296, 1995.

[34] Alexander V. Vologodskii and John F. Marko. Extension of torsionally stressed DNA by external force. *Biophysical Journal*, 73:123–132, 1997.

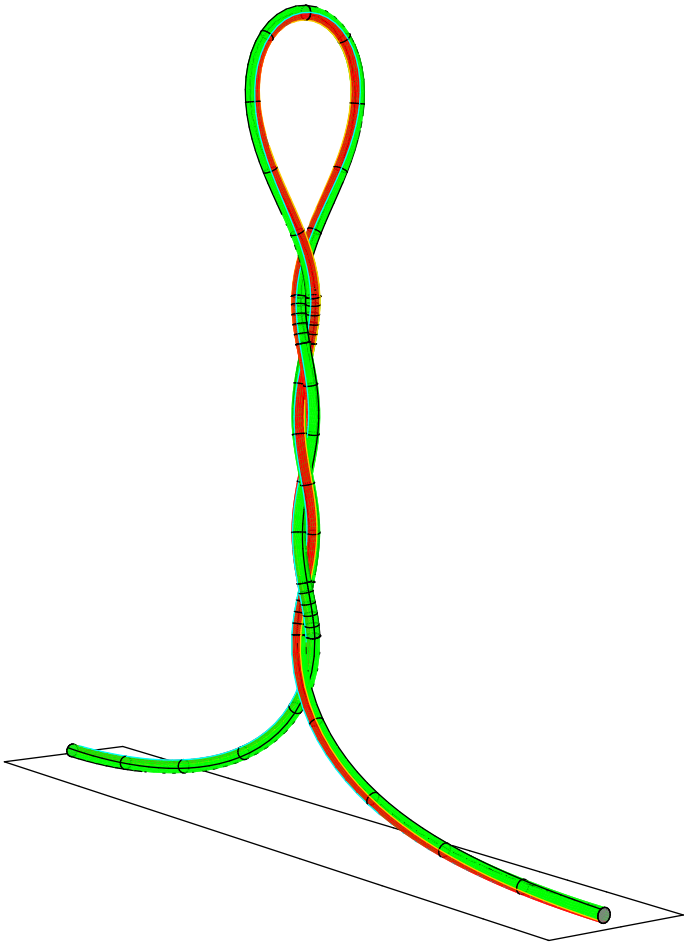

For Table of Contents use only
N. Clauvelin, B. Audoly, S. Neukirch
Mechanical response of plectonemic DNA: an analytical solution